

Analysis of Dislocation Mechanism for Melting of Elements: Pressure Dependence

Leonid Burakovsky*, Dean L. Preston[†] and Richard R. Silbar[‡]

Los Alamos National Laboratory
Los Alamos, NM 87545, USA

Abstract

In the framework of melting as a dislocation-mediated phase transition we derive an equation for the pressure dependence of the melting temperatures of the elements valid up to pressures of order their ambient bulk moduli. Melting curves are calculated for Al, Mg, Ni, Pb, the iron group (Fe, Ru, Os), the chromium group (Cr, Mo, W), the copper group (Cu, Ag, Au), noble gases (Ne, Ar, Kr, Xe, Rn), and six actinides (Am, Cm, Np, Pa, Th, U). These calculated melting curves are in good agreement with existing data. We also discuss the apparent equivalence of our melting relation and the Lindemann criterion, and the lack of the rigorous proof of their equivalence. We show that the would-be mathematical equivalence of both formulas must manifest itself in a new relation between the Grüneisen constant, bulk and shear moduli, and the pressure derivative of the shear modulus.

Key words: melting, string, dislocation, melting curve, equation of state, high pressure, elements, actinides

PACS: 62.50.+p, 64.10.+h, 64.70.Dv, 64.90.+b, 74.62.Fj, 77.84.Bw, 91.60.Gf

1 Introduction

The idea that a proliferation of dislocations is associated with melting dates back to Mott [1]. The very first theory of dislocation-mediated melting [2] was a success, inasmuch

*E-mail: BURAKOV@T5.LANL.GOV

[†]E-mail: DEAN@LANL.GOV

[‡]E-mail: SILBAR@WHISTLESOFT.COM. Also at WhistleSoft, Inc., Los Alamos, NM 87544, USA

as it predicted a first-order transition, as a consequence of incorporating the mutual screening of dislocations, in agreement with observations. Molecular dynamics [3] and Monte Carlo [4] calculations have more recently provided further evidence for the notion that dislocations drive the melting transition in three dimensions. There is also some experimental evidence that line defects are present in solids near melting [5].

In refs. [6, 7] we formulated a dislocation theory of melting in which dislocations near melt were modeled as non-interacting strings on a lattice. The possible configurations of a dislocation were taken to be closed random walks. Screening of long-range strain fields by other dislocations in a dense ensemble results in a $-\rho \ln \rho$ dependence of the free energy on the dislocation density, ρ , and thus a first-order transition. We obtained the following relation between the melting temperature T_m , the shear modulus, G , the Wigner-Seitz volume, v_{WS} , the coordination number, z , and the critical density of dislocations, $\rho(T_m)$ (in units where $k_B = 1$) :

$$T_m = \frac{\kappa \lambda G v_{WS}}{8\pi \ln(z-1)} \ln \left(\frac{\alpha^2}{4b^2 \rho(T_m)} \right). \quad (1)$$

Here b is the length of the shortest perfect-dislocation Burgers vector, κ is 1 for a screw dislocation and $(1-\nu)^{-1} \approx 3/2$ for an edge dislocation (ν is the Poisson ratio), $\lambda \equiv b^3/v_{WS}$ and α , which accounts for non-linear effects in the dislocation core, has a value of 2.9 [7]. Experimental data on 51 elements show that

$$\frac{G v_{WS}}{4\pi T_m \ln(z-1)} = 1.01 \pm 0.17 \quad (2)$$

at zero pressure [6]. Eqs. (1) and (2) imply that the critical dislocation density at zero pressure is

$$\rho(T_m) = (0.61 \pm 0.20) b^{-2}. \quad (3)$$

This value is in good agreement with the critical density

$$\rho(T_m) = (0.66 \pm 0.11) b^{-2}, \quad (4)$$

obtained by applying our relation for the latent heat of fusion [7],

$$L_m = \frac{1}{\lambda} b^2 \rho(T_m) R T_m \ln(z-1), \quad (5)$$

to data on latent heats for 75 elements. Hence, $b^2 \rho(T_m)$ is approximately constant across the Periodic Table with the numerical value

$$b^2 \rho(T_m) = 0.64 \pm 0.14, \quad (6)$$

which is the uncertainty-weighted average of Eqs. (3) and (4).

In this paper we investigate the validity of our melting relation, Eq. (1), up to pressures of order 100 GPa, by comparing to experimental melting curves, i.e., melting temperatures versus pressure, p . This comparison requires $v_{WS}(p)$, or its equivalent, the pressure dependence of the compression, $\eta \equiv V_0/V$. We obtain $\eta(p)$ from the bulk modulus, $B(p)$, which is extrapolated to high pressure using only its value and first pressure derivative at ambient conditions, viz., room temperature and zero pressure. The shear modulus $G(p)$

is similarly extrapolated to high pressure. Pressure derivatives of G and B are typically $O(1)$, so the extrapolation of the bulk modulus is expected to break down at pressures of order the ambient bulk modulus. The parameter κ in Eq. (1), which depends on the Poisson ratio, varies by only a few percent between $p = 0$ and 100 GPa (we discuss this in more detail in Section 2). Since the accuracy of our melting relation at zero pressure is 17%, we take κ to be a constant. We also make the necessary but reasonable assumption that $b^2\rho(T_m)$ is also a pressure-independent constant. With this assumption, we find that our melting relation agrees well with experimental melting curves up to pressures $\approx B$, and, in fact, our extrapolation of T_m is often in good agreement with data to pressures $\approx 2B$. In addition to the good agreement with the existing melting curve data, we also predict the high-pressure melting curves of Ag, Au, Cr, Cu, Mo, Os, Ru, W, and several actinides.

2 Melting curve equation

We now consider the pressure dependences of the factors appearing in our melting relation, Eq. (1). The parameter λ is constant by its definition, α is also assumed to be a constant, and κ may be taken as constant provided that the Poisson ratio ν has a very weak pressure dependence. In fact, for an isotropic medium [8]

$$\nu = \frac{1}{2} \frac{3B - 2G}{3B + G}. \quad (7)$$

Although both G and B vary with pressure, the ratio in Eq. (7) varies only weakly. Consider, for example, Cu, for which $\nu \approx 0.34$ at $p = 0$. At $p = 100$ GPa, we calculate the values of G and B with the help of Eqs. (13) and (14) below, with their pressure derivatives taken from ref. [9], and find $\nu \approx 0.38$. Therefore, in this case the corresponding values of $1/\kappa \approx 1 - \nu/2$ [7] are 0.83 and 0.81, respectively, so that the variation in the average value of $1/\kappa$ is $\approx 2\%$. Thus, the pressure dependence of $1/\kappa$ can be safely neglected. (There exists an upper bound on the change in the value of $1/\kappa$ with pressure. In the ultra-high-pressure limit, $p \propto \eta^{5/3}$, in agreement with the theory of the free electron gas (Fermi gas). Therefore, $B \equiv -Vdp/dV = \eta dp/d\eta \propto \eta^{5/3} \gg G \propto \eta^{4/3}$, and hence $\nu \rightarrow 1/2$, in view of Eq. (7) (see also [10]). Thus, in contrast to the Poisson ratio which changes by $\approx 50\%$, $1/\kappa \approx 1 - \nu/2$ changes by $\approx 10\%$: $5/6 \rightarrow 3/4$.)

We assume further that the mean interdislocation spacing at the melting point, $R \approx 1/\sqrt{\rho(T_m)}$, scales with b , independent of pressure, and hence $b^2\rho(T_m)$ is a pressure-independent constant (with a numerical value of 0.64 ± 0.14 , in view of Eq. (6)). It then follows from Eq. (1) that, provided the coordination number does not change with pressure (i.e., the element either remains in the same crystalline phase, or changes phase without changing the coordination number, e.g., a face-centered cubic structure \leftrightarrow a hexagonal close-packed structure), the melting relation is given by

$$\frac{G(p, T_m(p))v_{WS}(p, T_m(p))}{T_m(p)} = \text{const.} \quad (8)$$

The dependence of v_{WS} on pressure and temperature is just the equation of state of the metal. Let us first focus on its temperature dependence. The fixed-pressure ratio

of Wigner-Seitz volumes at T_m and $T = 0$ is equal to $1 + \beta T_m$, where β is the volume expansivity. At $p = 0$, β is typically of order 10^{-5} K^{-1} , and melting temperatures are at most about 4000 K, so v_{WS} changes by only a few percent between $T = 0$ and T_m . Assuming that β does not increase appreciably with compression, we can use room-temperature values for v_{WS} .

In contrast to v_{WS} , the dependence of G on T is not necessarily weak. Its T -dependence involves two characteristic temperatures, namely the Debye temperature, T_D , and the melting temperature. G is always monotonically decreasing with T , and is nonlinear for $T \lesssim T_D$ and linear from T_D to T_m . However, there are no experimental data, no computer calculations, and no theoretical guidance that tells us how the temperature dependence of G varies with pressure. In particular, how does the (negative) slope of the linear region vary with p ? At this point we have no choice but to conjecture. We assume that $G(p, T_m(p))/G(p, 0)$ is a slowly varying function of p , so it can be considered constant up to moderate compressions, say, 20% to 30%. Thus, $G(p, T_m)$ is replaced by $G(p, 0)$ in Eq. (8). In addition, data on the $p = 0$ temperature dependence of shear moduli [11] clearly show that $G(p, 300) \approx G(p, 0)$, and therefore, we use the room temperature value of the shear modulus in our melting relation.

Subsequently, the explicit dependence of G and v_{WS} on T will be dropped. It will be understood that G and v_{WS} are at room temperature. Our melting relation now reads

$$\frac{G(p)v_{WS}(p)}{T_m(p)} = \text{const.} \quad (9)$$

Differentiating Eq. (9) with respect to p , one finds

$$\frac{1}{T_m} \frac{dT_m}{dp} = \frac{1}{G} \frac{dG}{dp} - \frac{1}{B}, \quad (10)$$

where we have used the definition of the bulk modulus,

$$B(p) \equiv -V \frac{dp}{dV} = -v_{WS} \frac{dp}{dv_{WS}}. \quad (11)$$

Thus, upon integration, Eq. (10) gives

$$\frac{T_m(p)}{T_m(0)} = \frac{G(p)}{G(0)} \exp \left\{ - \int_0^p \frac{dp'}{B(p')} \right\}. \quad (12)$$

To proceed further, we have to specify $G(p)$ and $B(p)$.

2.1 The shear modulus G at finite pressure

For the shear modulus at all pressures, we use the relation [12]

$$G = G_0 + G'_0 \frac{p}{\eta^{1/3}}, \quad (13)$$

where $G'_0 \equiv (dG/dp)_0$. The subscript 0 refers to ambient conditions: $T \simeq 300 \text{ K}$ and $p = 0$.

This equation satisfies the requirement that $G \propto \eta^{4/3}$ as $\eta \rightarrow \infty$, since $p \propto \eta^{5/3}$. With the values of G'_0 for 32 elements tested in ref. [12] Eq. (13) gives nearly the right value for the proportionality constant between G and $\eta^{4/3}$ at high compressions. Eq. (13) works well for a diverse selection of engineering metals covering many different crystal structures and nearly all groups of the Periodic Table [12].

2.2 Compression and the bulk modulus B at finite pressure

Expanding the bulk modulus around $p = 0$ we have

$$B(p) = B_0 + B'_0 p + \frac{1}{2} B''_0 p^2 + \dots, \quad (14)$$

where B_0 and $B'_0 \equiv (dB/dp)_0$, $B''_0 \equiv (d^2B/dp^2)_0, \dots$ can be extracted from equation of state data. Values of B''_0 are known for a few elements only (their determination is highly uncertain and involves an error of order 100% [13]), and besides, B''_0 first appears in the $(p/B_0)^3$ term in the power series expansion of η :

$$\begin{aligned} \eta &= \exp \left\{ \int_0^p \frac{dp'}{B(p')} \right\} = \left[\frac{2B_0 + (B'_0 + \sqrt{B_0'^2 - 2B_0 B''_0})p}{2B_0 + (B'_0 - \sqrt{B_0'^2 - 2B_0 B''_0})p} \right]^{1/\sqrt{B_0'^2 - 2B_0 B''_0}} \\ &= 1 + \left(\frac{p}{B_0} \right) - \frac{B'_0 - 1}{2} \left(\frac{p}{B_0} \right)^2 + \frac{(B'_0 - 1)(2B'_0 - 1) - B_0 B''_0}{6} \left(\frac{p}{B_0} \right)^3 + \dots \end{aligned} \quad (15)$$

Since only B_0 and B'_0 are generally known (for almost all the elements, see ref. [9]), we restrict ourselves instead to the first two terms in Eq. (14). Then the compression simplifies to

$$\eta = \left(1 + \frac{B'_0}{B_0} p \right)^{1/B'_0}. \quad (16)$$

Eqs. (15) and (16) are two different approximations to the Murnaghan equation of state [14, 15].

It then follows from Eqs. (12), (13) and (16) that the equation of the melting curve is

$$T_m(p) = T_m(0) \left(1 + \frac{B'_0}{B_0} p \right)^{-1/B'_0} \left[1 + \frac{G'_0}{G_0} p \left(1 + \frac{B'_0}{B_0} p \right)^{-1/3B'_0} \right]. \quad (17)$$

As discussed in Section 4, this equation is only valid for pressures $p \lesssim 2B$.

It follows from (17) that for $p \ll B_0$

$$T_m(p) = T_m(0) \left[1 + \left(\frac{B_0 G'_0}{G_0} - 1 \right) \left(\frac{p}{B_0} \right) - \left(\frac{4}{3} \frac{B_0 G'_0}{G_0} - \frac{B'_0 + 1}{2} \right) \left(\frac{p}{B_0} \right)^2 + \dots \right]. \quad (18)$$

For the vast majority of the elements, $B'_0 > 5/3$ and B' approaches $5/3$ in the limit of large compressions. (In this limit $p \propto \eta^{5/3}$, and therefore $B \equiv -V dp/dV = \eta dp/d\eta = 5p/3$, i.e., $B' = 5/3$.) In fact, the average value of B'_0 for the 65 elements analyzed in [9], except for Ce for which $B'_0 < 0$, is 4.30 ± 1.40 . Hence, if

$$\frac{G'_0}{G_0} > \frac{3}{8} \frac{B'_0 + 1}{B_0}, \quad (19)$$

it follows from $B'_0 > 5/3$ that also $G'_0/G_0 > 1/B_0$, i.e., Eq. (18) is of the form $T_m(p) = T_m(0)(1 + ap - bp^2 + \dots)$, $a, b > 0$, and describes melting curves for which melting temperatures increase with pressure [16]. If, however,

$$\frac{G'_0}{G_0} < \frac{1}{B_0} \quad (20)$$

and $B'_0 > 5/3$, then also $G'_0/G_0 < 3/8 (B'_0 + 1)/B_0$, i.e., Eq. (18) is of the form $T_m(p) = T_m(0)(1 - ap + bp^2 - \dots)$, $a, b > 0$, and describes melting curves for which melting temperatures initially decrease with pressure [16]. For Si, for example, with the data from ref. [9] we find $G'_0/G_0 < 1/B_0$ and $B'_0 = 4.19$, in agreement with the negative initial slope of the experimental melting curve. Eqs. (19) and (20) plus $B'_0 > 5/3$ should be considered our criteria for the two types of melting curves discussed above.

3 Melting curves: comparison with data

In this section we compare our melting curve, Eq. (17), to some experimental melting curves, and predict a number of melting curves that can be compared with experiment in the not-so-distant future.

We have found 5 elements for which melting curves have been measured to higher pressures, $p \sim O(100 \text{ GPa})$: Al, Fe, Ni, Pb and U. We compare experimental data for these elements with our curves in Figs. 1-5. For Al, we also show the best fit to data in the form of the Simon equation, $T_m(p) = T_m(0)(1 + ap)^b$ [27]. For Fe, the experimental data are from ref. [28], and from ref. [29] for Ni. For Pb, we combine the high-pressure data of ref. [30] with the low-pressure data of ref. [31] as corrected in ref. [32]. For U, the high-pressure data of ref. [33] are combined with the low-pressure data of ref. [34].

As claimed in ref. [27], the Simon equation may not be the best functional form for a fit to data. In fact, the initial slope provided by this equation for the Al melting curve is 80 K/GPa, in contrast to 59 and 65 K/GPa from the two previous low-pressure measurements [27]. This accounts for the difference between the two curves in Fig. 1.

In Fig. 4, in addition to Fe, we also plot melting curves for Ru and Os, elements in the same column of the Periodic Table. Those curves should be considered predictions for these metals.

In Fig. 5, in addition to U for which there are high-pressure data, we also plot melting curves for the 5 actinides Am, Cm, Np, Pa and Th. For Np, we also show the low-pressure data of ref. [18]. We do not show the low-pressure data of ref. [17] for Am since they would overlay the low-pressure U data. We have checked that our melting curve is in agreement with the low-pressure Am data. For Cm, the values of B_0 and B'_0 are taken from ref. [35], and the value of G_0 is that estimated in ref. [6]. For Pa, the values of B_0 and G_0 come from ref. [8]. We estimate the values of G'_0 for Cm and Pa from Th and U, their neighbors in the same row in the Periodic Table. Our earlier G'_0 estimates for Am and Np lead to $\gamma = 1.05$ and 1.09 , respectively, in Eq. (24), which implies that such estimates are reliable. The values of B'_0 for Np and Pa are also estimated by interpolating between Am, Cm, Th and U. (We note that this estimation of B'_0 is justified by the pronounced periodic behavior of B'_0 in Z [36].) The value of B'_0 for Am is taken from [17]. We emphasize that the predicted melting curves assume constancy of coordination number along them. In the case of Am, e.g., there is still disagreement over the correct sequence of phases and their transition pressures [16], so this assumption may well be incorrect. For Th, however, it is claimed that there is a transition from a face-centered cubic structure to a body-centered tetragonal structure that changes coordination number [37]. This transition occurs in the pressure range of 70 – 100 GPa [37], and thus our predictions for the Th melting curve up to 75 GPa should be quite reliable.

Although we can account for a decrease in melting temperature with pressure in our

theoretical framework (Eqs. (17),(20)), we do not consider such cases here, among which there are Pu and Ce. It has been established [24] that for Th, which is in the same column as Ce, $\Delta V > 0$, and therefore, in view of Eq. (23), its melting temperature increases with pressure.

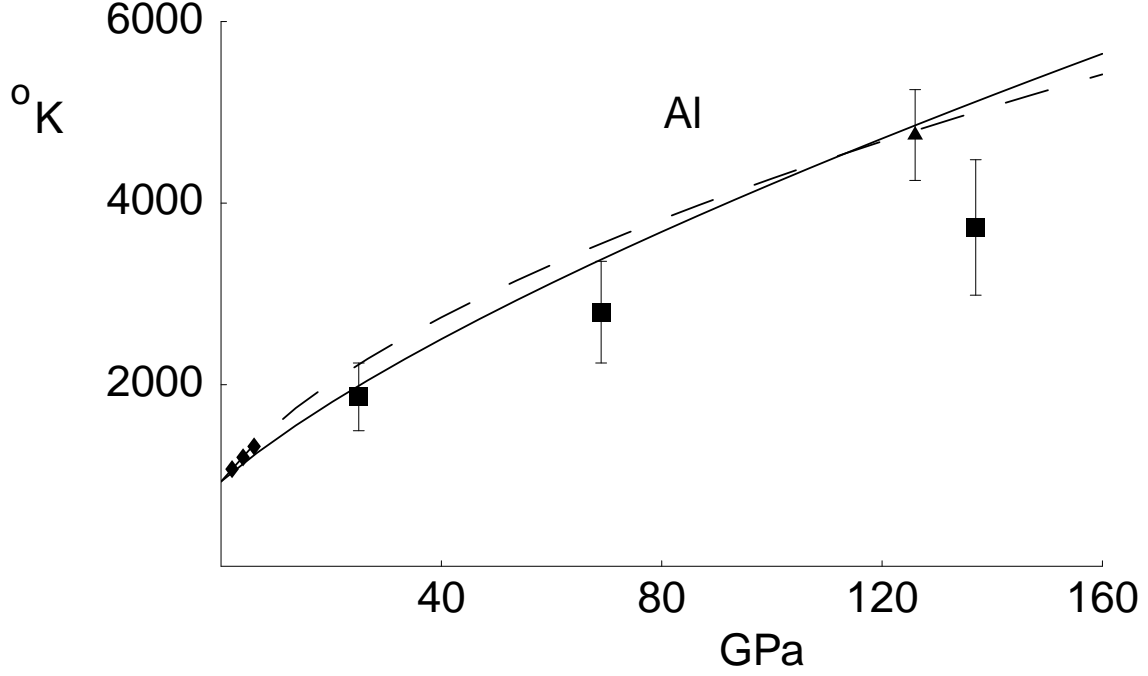


Fig. 1. Melting curve for Al. The dashed line is the Simon-fit to the data of ref. [27], which are not shown explicitly. The diamonds are the low-pressure data from ref. [38]. The triangle is the shock-melting point at 125 GPa from ref. [39]. The boxes are the points at 25, 69 and 137 GPa calculated in ref. [40] from shock-melting data. They are assigned 20% error bars [40].

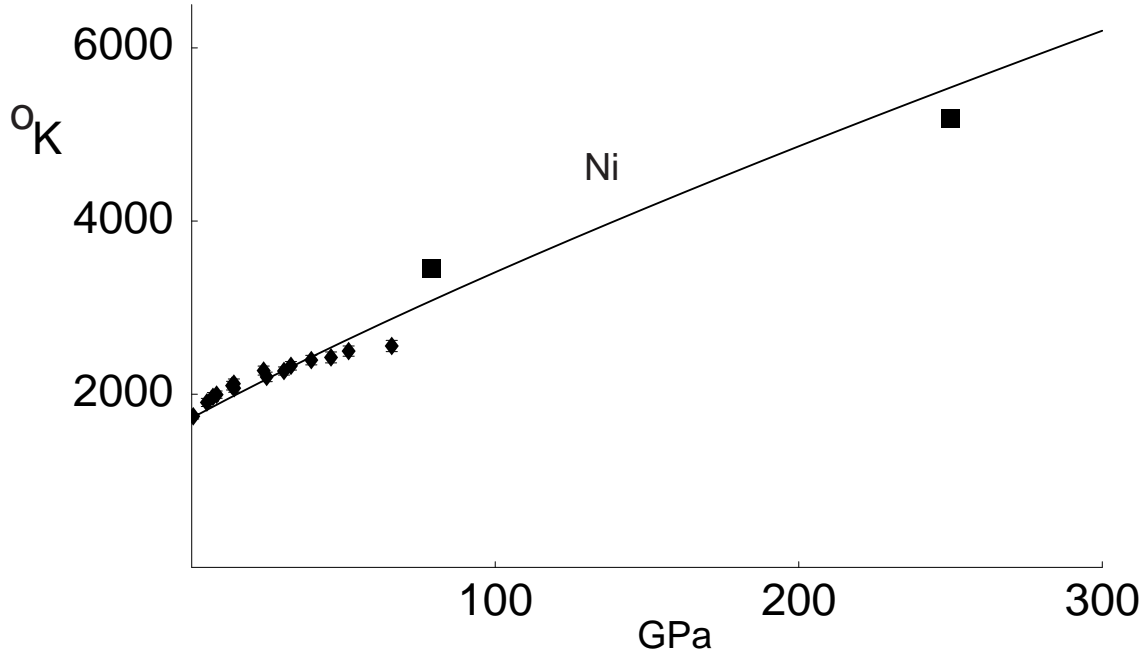


Fig. 2. Melting curve for Ni. The diamonds (with small error bars) are the data of ref. [29]. The boxes are the points at 79 and 250 GPa calculated in ref. [40] from shock-melting data. The corresponding error bars are not quoted in ref. [40].

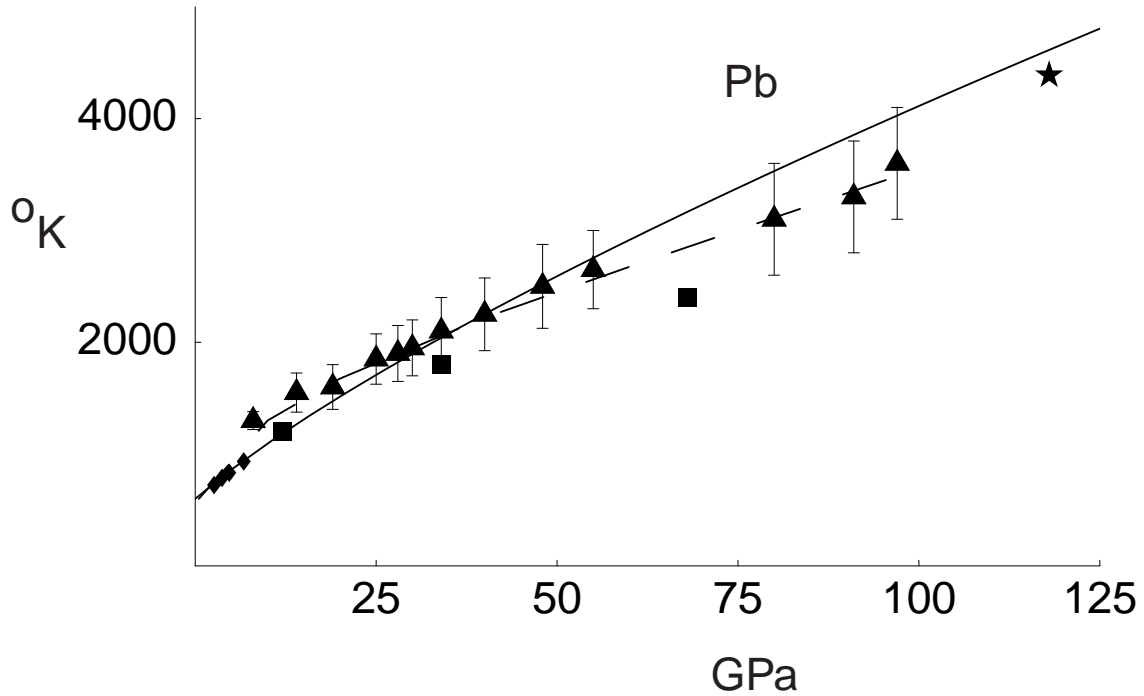


Fig. 3. Melting curve for Pb. The diamonds are the low-pressure data of ref. [31] corrected as in ref. [32]. The triangles are the data from ref. [30], and the dashed line is a best fit [30] to the data. The boxes are the points at 12, 34 and 68 GPa calculated in ref. [40] from shock-melting data. The corresponding error bars are not quoted in ref. [40]. The star is the point at 118 GPa calculated in ref. [41] from shock-melting data.

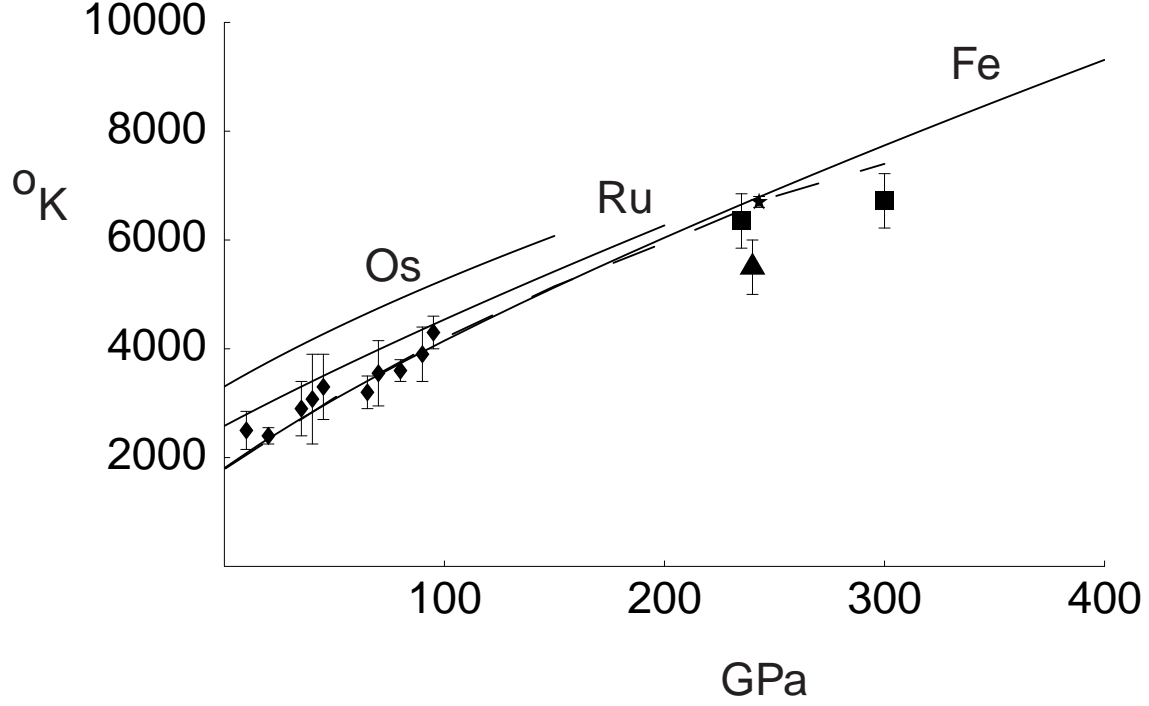


Fig. 4. Melting curves for the elements of the iron group (Fe, Ru, Os). The diamonds are the data of ref. [28], and the dashed line is a best fit [28] to the data. The boxes are the shock-melting points at 235 GPa and 300 GPa [42]. The triangle is the shock-melting point at 240 GPa [43]. The star is the shock-melting point at 243 GPa [44].

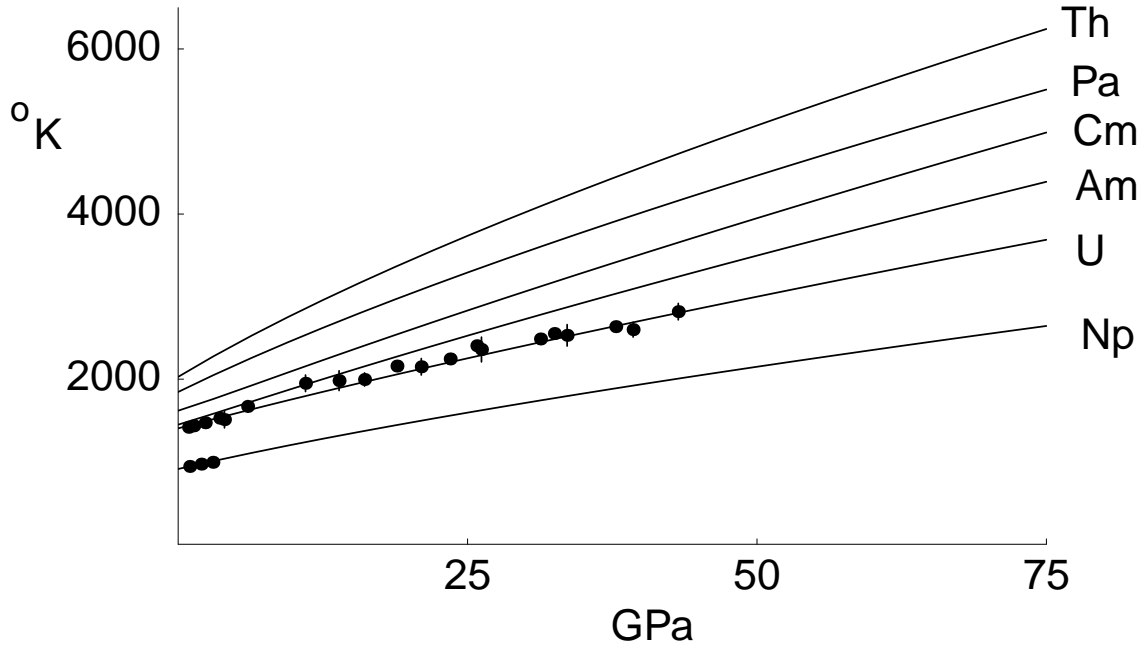


Fig. 5. Melting curves for the actinides Am, Cm, Np, Pa, Th and U. The data for U are from ref. [33], and for Np they come from ref. [18].

In Fig. 6 we plot the low-pressure data of ref. [25] for W, and our melting curves for W, Mo and Cr. The initial slope of our melting curve of Mo, 26 K/GPa, is consistent with that predicted in ref. [22]: (34 ± 6) K/GPa. The same melting curve gives $T_m \simeq 9650$ K at $p = 390$ GPa, in good agreement with the shock-melting temperature ~ 10000 K at the same pressure, found in ref. [45].

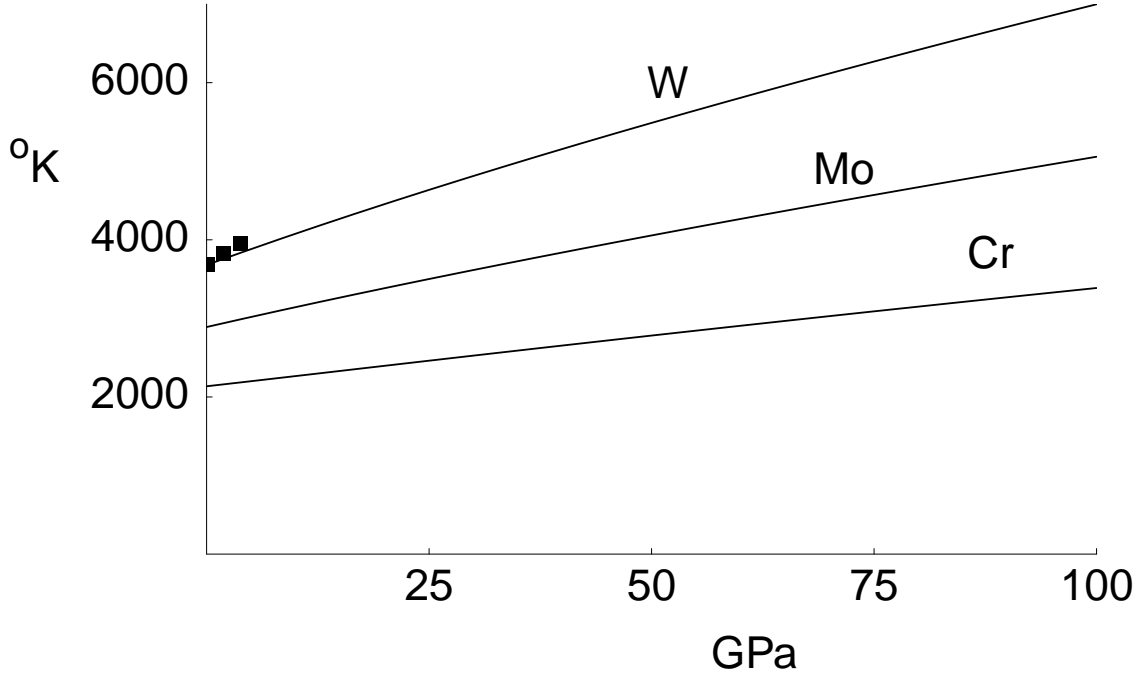


Fig. 6. Melting curves for the elements of the chromium group (Cr, Mo, W). The data for W are from ref. [25].

In Fig. 7 we compare the low-pressure data of ref. [46] for Cu, Ag and Au with our corresponding melting curves. Although the initial slopes of these curves are somewhat less than those of the data (the corresponding values of γ in Fig. 1 are $\simeq 0.8$), they are in good agreement with the best extrapolation of data to higher pressures made in ref. [46], and with the calculation of ref. [40] in the case of Cu.

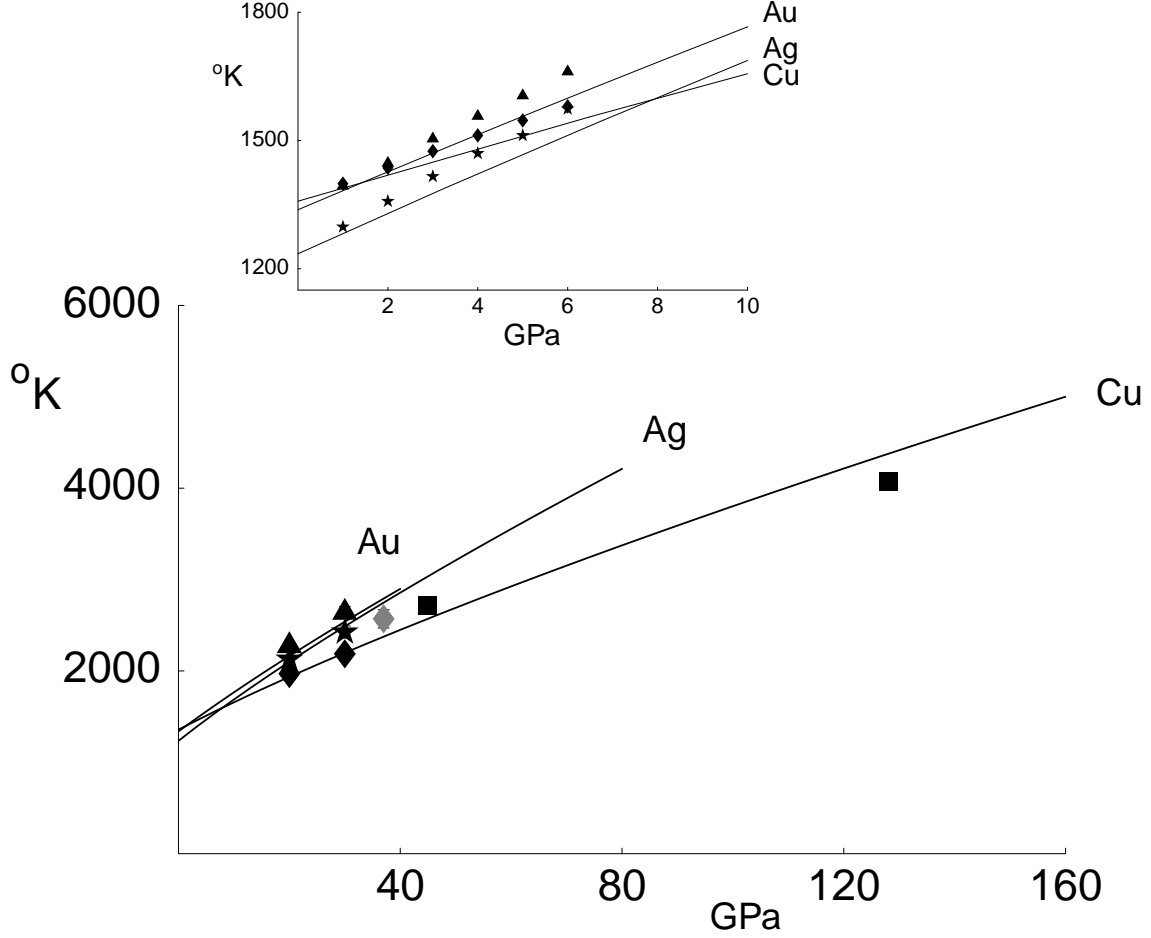


Fig. 7. Melting curves for the elements of the copper group (Cu, Ag, Au). The diamonds, the stars, and the triangles are the low-pressure data of ref. [46] in the inset, and the best extrapolations of these data to 20 and 30 GPa in the main plot for Cu, Ag and Au, respectively. The boxes are the points at 45 and 128 GPa calculated in ref. [40] from shock-melting data for Cu. The corresponding error bars are not quoted [40]. The gray diamond is the shock-melting point for Cu at 37 GPa [47].

In Fig. 8 we compare the low-pressure data on the noble gases to our corresponding melting curves. The unknown values of G'_0 for Ne, Ar, Kr and Xe are calculated with the help of Eq. (25) below using the measured values of B_0 , G_0 and γ_0 (the Grüneisen constant) [7]. The values of B'_0 for Ne, Ar, Kr and Xe are taken from [48]. In the case of Rn, for which B_0 , B'_0 , G_0 and G'_0 have not been measured, we first calculate G_0 using the (approximate) relation $GV/T_m = \text{const}$ for the noble-gas group, where $V = v_{WS}N_A$ is the molar volume. This relation follows from Eq. (1) provided that κ , λ , α and z do not vary within this group. The value of the constant is determined by using the corresponding Ne, Ar, Kr and Xe data in this relation. We then calculate B_0 using Eq. (7) with the value of the Poisson ratio for Rn determined by extrapolating from the corresponding values for Ne, Ar, Kr and Xe. Finally, we determine both B'_0 and G'_0 by again extrapolating the Ne, Ar, Kr and Xe data.

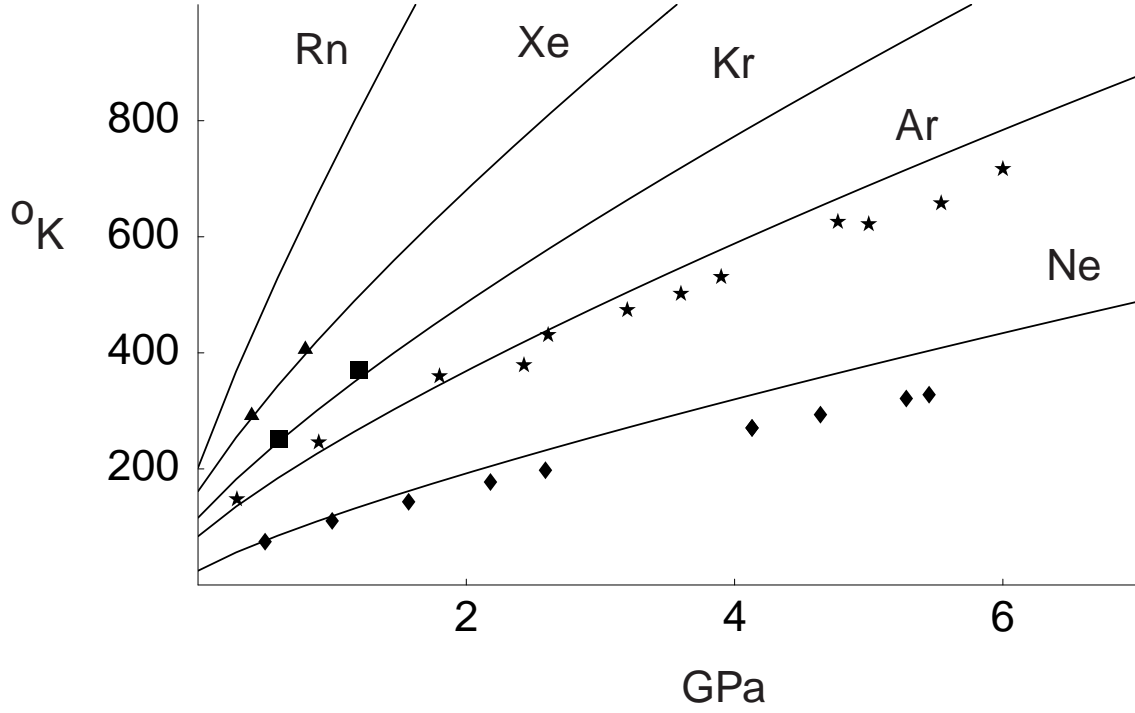


Fig. 8. Melting curves for the noble gases Ne, Ar, Kr, Xe and Rn. The diamonds are the data of ref. [49]. The stars are the data of ref. [50]. The boxes and triangles come from ref. [51].

Finally, in Fig. 9 we show the experimental data and our theoretical melting curve for Mg.

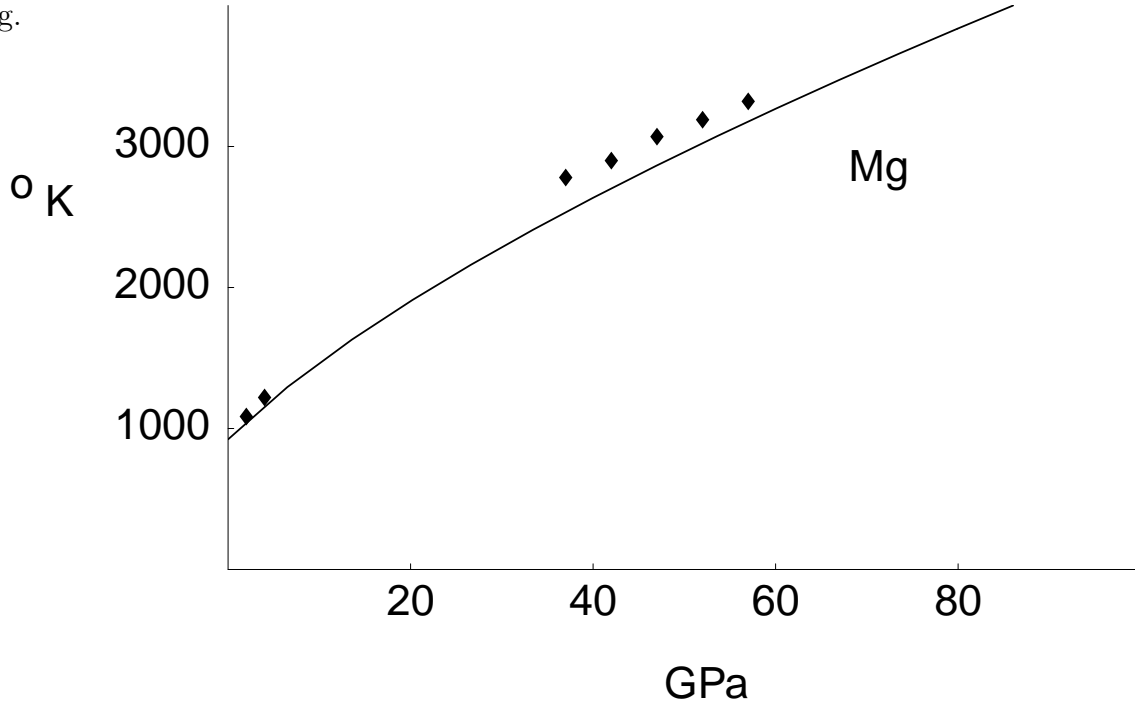


Fig. 9. Melting curve for Mg. The low-pressure data are from ref. [52]. The high-pressure data are the shock-melting points of ref. [53].

The 24 melting curves considered above constitute convincing evidence for the validity of our formula for melting temperature as a function of pressure, Eq. (17).

4 The range of validity of the new melting curve equation

In deriving our melting curve, Eq. (17), we have used both Eq. (13) for the pressure dependence of the shear modulus and the Murnaghan equation of state, Eq. (16). Since Eq. (13) has the correct zero-pressure limit (its Taylor series expansion in p at $p = 0$ is $G = G_0 + G'_0 p - (G'_0/3B_0)p^2 + \dots$) and is claimed to have the correct ultra-high-pressure limit [12], we assume that this equation is valid over the entire pressure range. In any event, we do not have data to either confirm or invalidate this assumption. It then follows that the range of validity of Eq. (17) depends crucially on the range of validity of the Murnaghan equation of state, Eq. (16).

The Murnaghan equation of state was examined in ref. [15], together with a number of different equations of state, by comparing with the theoretical results calculated by the augmented-plane-wave method and the quantum-mechanical model proposed by Kalitkin and Kuz'mina [54] from low to ultra-high pressures. It was shown that the Murnaghan equation is in good agreement with the theoretical results up to $V/V_0 \simeq 0.7$, i.e., up to compressions $\simeq 1.4 - 1.5$. Since for the vast majority of the elements $B'_0 \approx 5$ [9], we conclude, on the basis of Eq. (16), that the Murnaghan equation, and consequently, our equation for melting curve, Eq. (17), is valid up to pressures $p \approx 2B_0$. The melting curves for Al and Pb in Figs. 1 and 3, respectively, and for Ne and Ar in Fig. 8 show that in some cases Eq. (17) is good to pressures even greater than $2B_0$.

For reliable predictions of melting curves to much higher pressures, $p \gtrsim 1$ TPa, one has to use a better equation of state than Murnaghan's. Hama and Suito [15] claim that the Vinet equation of state [55] is consistent with first-principles theoretical calculations to compressions $\eta \sim 5$. Reference [56] also finds the Vinet equation of state to be most accurate among various suggested equations of state. In fact, we have calculated that the melting temperatures for Fe and Pb at pressures $p \sim 50 B_0$ as given by Eq. (17) are about two times higher than those given by a relation that derives from Eqs. (12), (13), and the Vinet equation of state.

Another possible source of disagreement between the new melting curve, Eq. (17), and data may be inaccurate values of elastic constants and their pressure derivatives in some cases. The Murnaghan equation and its frequently used partner – the Birch equation [57] – are derived from the second-order Taylor series expansion of the bulk modulus [as in Eq. (14)] or the elastic strain energy with respect to pressure or strain, respectively. Thus their validities are, in principle, restricted to a narrow range of compression. Extending this range would entail the inclusion of higher-order terms. This could explain why the values of B_0 , and especially those of B'_0 and B''_0 , obtained from experiments which cover different ranges of compression by using a fitting method, are usually different. In many cases these differences between different experiments are small and can be safely neglected. In some cases, however, they are large, and so their use for predicting physical observables, such as melting temperature, is dubious. For example, in the case of Ni, we have used the value $B'_0 = 6.20$ given in [9]. Reference [58], however, quotes $B'_0 \simeq 30$ (!). Similarly, for Mo we

have used $B'_0 = 4.4$ of ref. [9], while ref. [58] gives $B'_0 \simeq 20$. (We note that the use of the values $B'_0 = 6.20$ for Ni and 4.4 for Mo is justified in view of the recent compilations of experimental data on B'_0 [59].) Although the numerical value of B'_0 does not matter at low p , since it first appears in the $(p/B_0)^2$ term, in view of Eq. (15), it would strongly affect the predicted melting curve at pressures $p \sim O(B_0)$.

There are also inconsistencies in the values of G_0 quoted in the literature. For example, for Pb we use the value $G_0 = 8.6$ GPa from ref. [9], whereas ref. [8] quotes $G = 5.5$ GPa. (Our own calculation [6], based on the values of the elastic constants c_{11} , c_{12} and c_{44} , shows that 8.6 GPa is preferred over 5.5 GPa.) Likewise the values of G_0 for K and Na from ref. [9] are 0.9 and 1.98 GPa, whereas ref. [8] quotes 1.3 and 3.5 GPa, respectively.

5 Relation of dislocation-based melting relation to the Lindemann criterion

The well-known Lindemann melting rule is based on the assumption that all elemental solids melt when the atomic vibrational amplitude is a fixed pressure-independent fraction of the interatomic distance. As shown by Lindemann [60], this implies the invariance of the Lindemann number

$$\theta_D \left(\frac{M}{T_m} \right)^{1/2} V^{1/3} = L \quad (21)$$

along the melting curve. Here θ_D is the density-dependent Debye temperature, V is the molar volume, and M is the molar mass. It is found that $L \approx 150$ [8].

There are compelling reasons to suppose that our dislocation-based melting relation is somehow equivalent to the Lindemann criterion. First of all, Eq. (21) gives melting curves that are typically very close to those predicted by our dislocation-based melting relation. (For example, the melting curve for Mg in Fig. 6.3 of ref. [16] is *very* similar to our curve in Fig. 9.) Furthermore, the Lindemann number, which is proportional to the ratio of atomic vibrational amplitude to the lattice constant at melt, is analogous to $b^2 \rho(T_m)$, since both are presumed constant along the melting curve. In the dislocation-based approach, melting is associated with a critical configuration of dislocations, and for any such configuration there is a corresponding mean displacement of atoms from their equilibrium positions. Hence L and $b^2 \rho(T_m)$ are clearly related, and therefore the left-hand sides of Eqs. (9) and (21) are related as well.

The mathematical equivalence of our melting relation and the Lindemann criterion would be established if it could be determined that the left-hand side of Eq. (21) is a fixed fraction of the left-hand side of Eq. (9). A search of the literature has turned up two results which show that L^2 is *approximately* proportional to Gv_{WS}/T_m . For a Debye solid the relation is [61] $L^2 = f(\nu(p, T))Gv_{WS}/T_m$, where f is a complicated function of ν . Thus the two melting relations are not rigorously equivalent.

A second connection between the two melting formulas is provided by the following approximation for the Grüneisen constant [9],

$$\gamma(p) = \frac{2}{3} \gamma_S(p) + \frac{1}{3} \gamma_L(p), \quad (22)$$

where

$$\gamma_S(p) = \frac{G'(p)}{2} \frac{B^T(p)}{G(p)} - \frac{1}{6}, \quad (23)$$

$$\gamma_L(p) = \frac{1}{2} \frac{B^T(p)}{B^S(p) + \frac{4}{3}G(p)} \frac{d(B^S(p) + \frac{4}{3}G(p))}{dp} - \frac{1}{6}, \quad (24)$$

are the contributions of the shear (transverse) and longitudinal acoustic modes. Here B^T is the isothermal bulk modulus, which is equivalent to B that we are using in this paper. Eqs. (22)-(24) follow from the two assumptions that (i) the only appreciable contribution to the heat capacity of a crystal arises from lattice vibrations, and (ii) averaging over all modes is equivalent to averaging only over the low-frequency acoustic modes. (I.e., the contribution of the optical modes is equal to that of the acoustic modes.) If in addition it is assumed that $B^S(p)$, the isentropic bulk modulus, is proportional to $G(p)$, then

$$\gamma_S(p) = \gamma_L(p) = \gamma(p) = \frac{G'(p)}{2} \frac{B(p)}{G(p)} - \frac{1}{6}. \quad (25)$$

However, there is no basis for this assumption, i.e., $\gamma_S(p) \neq \gamma_L(p)$ is to be expected. For example, in the ultra-high pressure limit, $B^S(p) \sim B^T(p) = 5p/3$ and $G(p) \sim p^{4/5}$, quite different dependencies.

Integration of Eq. (25), using $B(p) = -dp/d \ln V(p)$ and $\gamma(p) = -d \ln \theta_D(p)/d \ln V(p)$, gives

$$\frac{\theta_D^2(p) V^{2/3}(p)/T_m(p)}{G(p) V(p)/T_m(p)} = \text{const}, \quad (26)$$

that is, $L^2 \propto G v_{WS}/T_m$. We emphasize that this proportionality is founded on a number of uncontrolled approximations.

Equation (25), which would ensure a rigorous mathematical equivalence of the defect and mechanical (Lindemann's) approaches to melting, does *not* follow from first principles. This means that the defect and mechanical approaches to melting are basically *different*. Moreover, since the mechanical approach does not have a solid thermodynamic basis, it cannot, for example, predict the latent heat of fusion. In contrast, the defect approach predicts the latent heat of fusion, Eq. (9), which is in good agreement with data for three-quarters of the Periodic Table [7].

Finally, we wish to make the following comments on Eq. (25). We did not check extensively its validity at zero pressure, since that would go beyond the scope of this paper. We do, however, have some evidence that Eq. (25) is rather well satisfied: with the data from ref. [9], we calculate from the above relation $\gamma_0 = 2.25$ vs. measured 2.40 for Ag, 3.08 vs. 2.99 for Au, 1.66 vs. 1.78 for Fe, 1.28 vs. 1.29 for K, and 1.18 vs. 1.19 for Na. We have actually used Eq. (25) in Section 3 to calculate G'_0 for noble gases in order to get their melting curves via Eq. (17) and to compare with experiment. Good agreement between the calculated and experimental curves is another hint on the approximate validity of this formula. Also, Eq. (25) has the correct ultra-high-pressure limit in which $\gamma \rightarrow 1/2$ [10], since in this limit $G \sim p^{4/5}$ and $B = 5p/3$.

6 Concluding remarks

We have extended the framework of melting as a string-mediated phase transition to non-zero pressure and derived a new equation for the melting curve, Eq. (17). As discussed above, with accurate experimental values of all the parameters involved, this equation reproduces the existing experimental melting data, and predicts unknown melting curves to pressures $p \lesssim 2B_0$. For higher pressures, a better equation of state than Murnaghan's should be used, e.g., the Vinet equation of state.

We have addressed the apparent equivalence of defect and mechanical approaches to melting curve, and demonstrated that both approaches are basically different. We have shown that their would-be rigorous mathematical equivalence must manifest itself in a new relation, Eq. (25), which we have not tested in detail.

To summarize, we have calculated melting curves for 24 elements: Al, Mg, Ni, Pb, the iron group (Fe, Ru, Os), the chromium group (Cr, Mo, W), the copper group (Cu, Ag, Au), the noble gases Ne, Ar, Kr, Xe and Rn, and the six actinides Am, Cm, Np, Pa, Th and U. These calculated melting curves are in good agreement with existing data.

Acknowledgements

We wish to thank T. Goldman and A.Z. Patashinski for valuable discussions during the preparation of this work. One of us (L.B.) wishes to thank B.K. Godwal for useful correspondence.

References

- [1] C. Mott, Proc. Roy. Soc. A **215** (1952) 1
- [2] S. Mizushima, J. Phys. Soc. Japan **15** (1960) 70
A. Ookawa, J. Phys. Soc. Japan **15** (1960) 2191
- [3] R.M.J. Cotterill, Phys. Rev. Lett. **42** (1979) 1541
- [4] W. Janke, Int. J. Theor. Phys. **29** (1990) 1251
L. Gómez, A. Dobry and H.T. Diep, Phys. Rev. B **55** (1997) 6265
- [5] R.K. Crawford, Bul. Am. Phys. Soc. **24** (1979) 385
R.M.J. Cotterill and J.K. Kristensen, Phil. Mag. **36** (1977) 453
Y. Wang and K. Kakimoto, J. Crystal Growth **208** (2000) 303
- [6] L. Burakovsky and D.L. Preston, Analysis of dislocation mechanism for melting of elements, Los Alamos preprint LA-UR-99-4171 [cond-mat/0003494], Solid State Comm., *in press*
- [7] L. Burakovsky, D.L. Preston and R.R. Silbar, Melting as a string-mediated phase transition, Los Alamos preprint LA-UR-99-5914 [cond-mat/0004011], Phys. Rev. B, *in press*

- [8] K.A. Gschneidner, Jr., in *Solid State Physics, Advances in Research and Applications*, Eds. F. Seitz and D. Turnbull, (Academic Press, New York, 1965), Vol. 16, p. 275
- [9] M.W. Guinan and D.J. Steinberg, J. Phys. Chem. Solids **35** (1974) 1501
- [10] V.P. Kopyshchev, Sov. Phys. Doklady **10** (1965) 338
- [11] G. Simmons and H. Wang, *Single Crystal Elastic Constants and Calculated Aggregate Properties*, 2nd ed., (MIT Press, Cambridge, MA, 1971)
- [12] M. Guinan and D. Steinberg, J. Phys. Chem. Solids **36** (1975) 829
- [13] J. Freund and R. Ingham, J. Phys. Chem. Solids **50** (1989) 263
- [14] F.D. Murnaghan, Proc. Nat. Acad. Sci. US **30** (1944) 244
- [15] J. Hama and K. Suito, J. Phys.: Cond. Mat. **8** (1996) 67
- [16] D.A. Young, *Phase Diagrams of the Elements*, (University of California Press, Berkeley, 1991)
- [17] D.R. Stephens, H.D. Stromberg and E.M. Lilley, J. Phys. Chem. Solids **29** (1968) 815
- [18] D.R. Stephens, J. Phys. Chem. Solids **27** (1966) 1201
- [19] E.Yu. Tonkov, *High Pressure Phase Transformations*, (Gordon and Breach, Philadelphia, 1992)
- [20] A.R. Ubbelohde, *The Molten State of Matter*, (Wiley, New York, 1978)
- [21] G.R. Gathers, J.W. Shaner, R.S. Hixson and D.A. Young, High Temp.-High Press. **11** (1979) 653
- [22] J.W. Shaner, G.R. Gathers and C. Minichino, High Temp.-High Press. **9** (1977) 331
- [23] W.M. Hodgson, Ph.D. thesis (Lawrence Livermore preprint UCRL-52493 (1978))
- [24] M. Boivineau, H. Colin, J.M. Vermeulen and Th. Thévenin, Int. J. Thermophys. **17** (1996) 1001
- [25] A. Kloss, H. Hess, H. Schneidenbach and R. Grossjohann, Int. J. Thermophys. **20** (1999) 1199
- [26] J.A. Moriarty, D.A. Young and M. Ross, Phys. Rev. B **30** (1984) 578
- [27] R. Boehler and M. Ross, Earth Plan. Sci. Lett. **153** (1997) 223
- [28] Q. Williams, R. Jeanloz, J. Bass, B. Svedensen and T.J. Ahrens, Science **236** (1987) 181
- [29] P. Lazor, G. Shen and S.K. Saxena, Phys. Chem. Min. **20** (1993) 86

- [30] B.K. Godwal, C. Meade, R. Jeanloz, A. Garcia, A.Y. Liu and L. Cohen, *Science* **248** (1990) 462
- [31] P.W. Mirwald and G.C. Kennedy, *J. Phys. Chem. Solids* **37** (1976) 795
- [32] M. Akaishi, H. Kanda, N. Setaka and O. Fukunaga, *Japan J. Appl. Phys.* **16** (1977) 1077
- [33] C.S. Yoo, J. Akella and J.A. Moriarty, *Phys. Rev. B* **48** (1993) 15529
- [34] J. Ganguly and G.C. Kennedy, *J. Phys. Chem. Solids* **34** (1973) 2272
- [35] R.G. Haire, U. Benedict, J.R. Peterson, C. Dufour and J.P. Itié, *J. Less-Common Met.* **109** (1985) 71
- [36] D.J. Steinberg, *J. Phys. Chem. Solids* **43** (1982) 1173
- [37] Y.K. Vohra and J. Akella, *Phys. Rev. Lett.* **67** (1991) 3563
K. Ghandehari and Y.K. Vohra, *Scr. Metal. Mater.* **27** (1992) 195
- [38] J. Lees and B.H.J. Williamson, *Nature* **208** (1965) 278
- [39] J.M. Shaner, J.M. Brown and R.G. McQueen, in *High Pressure in Science and Technology*, Eds. C. Homan, R.K. MacCrone and E. Whalley, (North Holland, Amsterdam, 1984), p. 137
- [40] V.D. Urlin, *Zh.E.T.F.* **49** (1965) 485
- [41] B.K. Godwal, S.K. Sikka and R. Chidambaram, *Pramana* **29** (1987) 93. The typo in the value of T_m (118 GPa) found by us was communicated with B.K. Godwal.
- [42] C.S. Yoo, N.C. Holmes, M. Ross, D.J. Webb and C. Pike, *Phys. Rev. Lett.* **70** (1993) 3931
- [43] J.M. Brown and R.G. McQueen, *J. Geophys. Res.* **91** (1986) 7485
- [44] J.D. Bass, in *High Pressure Research in Mineral Physics*, Eds. M.H. Manghnani and Y. Syono, (Terra Scientific, Tokyo, 1987), p. 393
- [45] R.S. Hixson, D.A. Boness, J.W. Shaner and J.A. Moriarty, *Phys. Rev. Lett.* **62** (1989) 637
- [46] P.W. Mirwald and G.C. Kennedy, *J. Geophys. Res.* **84** (1979) 6750
- [47] A.I. Funtikov, *Fiz. Goreniya Vzryva* **5** (1969) 510
- [48] *Rare Gas Solids*, Eds. M.L. Klein and J.A. Venables, (Academic Press, London, 1977), Vol. II, Chapter 13
- [49] W.L. Vos, J.A. Schouten, D.A. Young and M. Ross, *J. Chem. Phys.* **94** (1991) 3835
- [50] C.-S. Zha, R. Boehler, D.A. Young and M. Ross, *J. Chem. Phys.* **85** (1986) 1034

- [51] P.H. Lahr and W.G. Eversole, J. Chem. Eng. Data **7** (1962) 42
- [52] G.C. Kennedy and R.C. Newton, in *Solids under Pressure*, Eds. W. Paul and D.M. Warschauer, (McGraw-Hill, New York, 1963), p. 163
- [53] P.A. Urtiew and R. Grover, J. Appl. Phys. **48** (1977) 1122
- [54] N.N. Kalitkin and L.V. Kuz'mina, Sov. Phys. Solid State **13** (1972) 1938
- [55] P. Vinet, J. Ferrante, J.R. Smith and J.H. Rose, J. Phys. C **19** (1986) L467
P. Vinet, J. Ferrante and J.H. Rose, Phys. Rev. B **35** (1987) 1945
- [56] R.E. Cohen, O. Gülseren and R.J. Hemley, Amer. Mineral. **85** (2000) 338
- [57] F. Birch, J. Geophys. Res. **57** (1952) 227, **83** (1978) 1257
- [58] L. Gerward, J. Phys. Chem. Solids **46** (1985) 925
- [59] Z.-H. Fang and L.-R. Chen, Phys. Stat. Sol. B **180** (1993) K5
S. Raju, E. Mohandas and V.S. Raghunathan, J. Phys. Chem. Solids **58** (1997) 1367
- [60] F.A. Lindemann, Phys. Z. **11** (1910) 609
- [61] H. Kleinert, *Gauge Fields in Condensed Matter*, (World Scientific, Singapore, 1989), Vol. II